# Experimental Study about internal Cavitating Flow and Primary Atomization of a Large-Scaled VCO Diesel Injector with Eccentric Needle

T. Oda[1,*], Y. Goda[1], S. Kanaike[2], K. Aoki[3] and K. Ohsawa[1]
[1] Department of Mechanical Engineering, Tottori University, Koyama 4-101, TOTTORI 680-8552 JAPAN
[2] Mitsubishi Motors Corporation
[3] West Japan Railway Company

**Abstract**

This paper describes an experimental study to investigate the effects of eccentricity of a needle inside a valve-covered-orifice (VCO) diesel nozzle on internal cavitating flow and primary atomization, so a 10 times large-scaled VCO nozzle was employed. The needle, which was incorporated into the nozzle, was manipulated by a three-dimensional traverse with micrometers. When the needle is located around the nozzle center, the spray cone angle remains almost constant at relatively high needle lift. However at relatively low needle lift various behaviors are observed as follows: when the needle is positioned along the nozzle hole, the significant increase of spray cone angle is observed around the nozzle center. On the other hand, when the needle is perpendicularly positioned to the nozzle hole, the tendency of the spray cone angle is very complicated because of cavitating flow behavior inside nozzle hole, in addition to the relatively high spray cone angle. In this geometric condition the cavitating flow inside the nozzle hole can be classified into four regimes while two regimes, the hollow cone spray regime and the solid cone spray regime, can be obtained as jet breakup. The radial locations of the four regimes hardly depend on the injection pressure. Additionally the value of the discharge coefficient is less dependent on the injection pressure while the spray cone angle is strongly affected by the injection pressure.

## Introduction

The valve-covered-orifice (VCO) nozzles are usually employed in order to reduce unburned hydrocarbon emissions of diesel engines. However some researchers [1,2,3,4] have qualitatively demonstrated that different size sprays were ejected from real-size VCO nozzle because of eccentric location of needle incorporated into the nozzle. As a result, asymmetric combustion and soot formation are caused [1].

The large-scaled nozzles have been employed frequently under steady-state condition with constant injection pressure, constant back pressure and constant needle lift, so that cavitation bubbles and resulting sprays could have been easily observed [5,6]. Especially, string-like bubbles, so called the vortex cavitation bubbles, and hollow cone sprays have been observed at very low needle lifts. We performed a steady-state experiment by using a 10 times large-scaled VCO nozzle with good spatial resolution of a 3-D traverse to manipulate a needle, and the experimental study provided quantitative information that the asymmetric location of needle influences flow patterns inside the nozzle and structures of resulting liquid jets [7]. This experimental study seems to suggest that axial momentum and angular momentum of internal flow might play an important role in the flow pattern and the structures of liquid jets. The axial momentum and the angular momentum might strongly relate to discharge coefficient of the nozzle.

This paper represents patterns of internal cavitating flows, structures of liquid jets, spray cone angles and discharge coefficients of our original VCO nozzle [7] in terms of eccentricity of the needle.

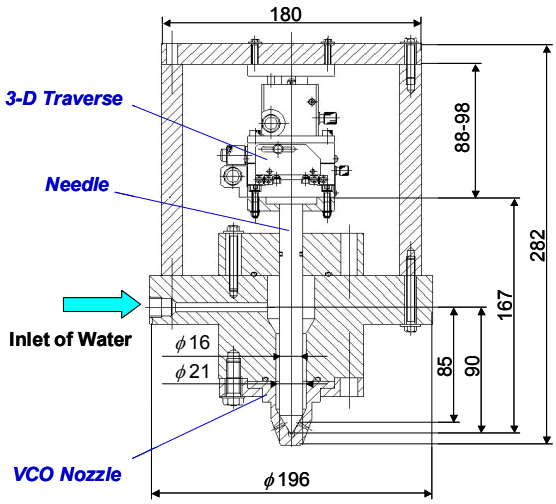


**Figure 1.** Schematic of nozzle holder with 10 times large-scaled VCO nozzle.

*Corresponding author: odate@mech.tottori-u.ac.jp

## Experimental Procedure

An accumulator containing water, which was employed as the test liquid, was pressurized by an air compressor up to 1.2MPa. A pressure regulator was used to maintain the pressure in the accumulator. The liquid from the accumulator passed steadily through a needle valve and a Bourdon-type pressure gauge, which were used to control the injection pressure, before the liquid attained a nozzle holder, which is shown in Fig. 1. The liquid introduced into an inlet of the nozzle holder before flowing a pre-nozzle region which was located just upstream of a seat. A needle was incorporated into the nozzle holder, and had a diameter of 16mm and a 60°-edge tip. A large-scaled VCO nozzle, which was made of transparent acrylic resin, was mounted downstream of the nozzle holder. Finally the liquid was ejected from nozzle holes to the quiescent atmospheric air. The needle was mounted underneath the 3-D traverse with three micrometers which could provide a minimum resolution of 10μm. The needle lift and the eccentric radial location were set in terms of the micrometers reading before the liquid was emerged.

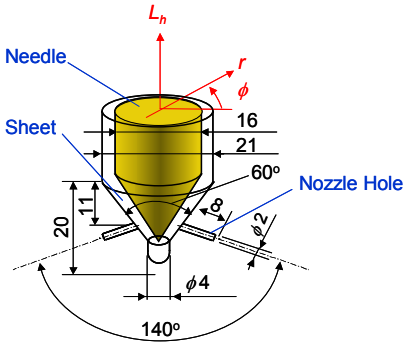


(a) Nozzle geometry and coordinate system.

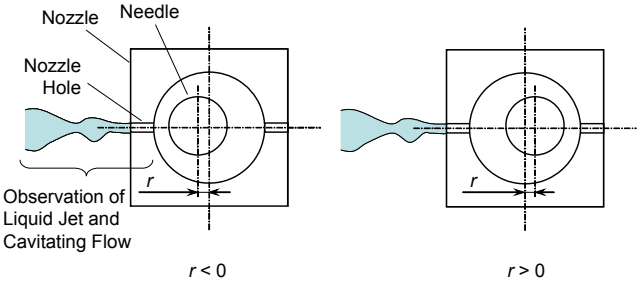


(b) Radial location of needle at azimuthal angle of 0°

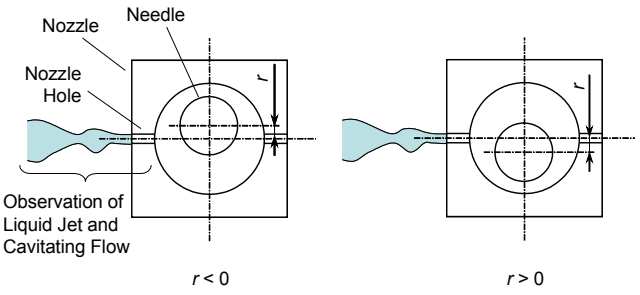


(c) Radial location of needle at azimuthal angle of 90°

**Figure 2.** Schematic of nozzle geometry and coordinate system.

The large-scaled VCO nozzle had two nozzle holes as illustrated in Fig. 2 (a). Both the nozzle holes had sharp-edged circular shape at the entrance of the holes. The diameter of both the nozzle holes was 2mm and the length was 8mm, providing a length to diameter ratio of 4. The large-scaled VCO nozzle was ten times larger than real-size diesel nozzles. At an injection pressure of 0.20MPa the Reynolds number of the flow inside the nozzle hole of the large-scaled VCO nozzle was achieved at maximum Reynolds number of approximately 40000. The maximum Reynolds number of the large-scaled VCO nozzle was nearly the same value as that of real-size diesel nozzles.

The needle lift and the radial location denote $L_h$ and $r$, respectively. $\phi$ describes the azimuthal angle from common plane of the two holes axes. However our coordinate system is different from conventional cylindrical coordinate system. Figures 2 (b) and (c) explain radial locations at the azimuthal angle of 0° and 90°, respectively. The radial location which has negative value is opposed to that which has positive value in our coordinate system. There exists the radial location along the direction of the nozzle holes at the azimuthal angle of 0° (Fig. 2 (b)). As the value of the radial location decreases at the azimuthal angle, the needle approaches the entrance of the nozzle hole for observation.

Cavitating bubbles inside the nozzle and liquid jet were illuminated simultaneously by two Xenon flashes of 4μs duration. Therefore front-lit photographs of cavitating bubbles and the liquid jet were captured by a digital still camera. Behaviors of the cavitating flow and the liquid jet breakup could be observed from each photograph, and spray cone angle was estimated by using the photograph.

## Results and Discussion

Figure 3 illustrates the spray cone angles at the azimuthal angle of $\phi$=0°. At the high needle lift of $L_h$=3.00mm the spray cone angle increases with increasing the value of the radial location up to about $r$=-1.3mm, and then reduces up to about $r$=-0.80mm. Further increase beyond $r$=-0.80mm causes the spray cone angle to remain constant value. At the low needle lift of $L_h$=0.50mm measuring range of the radial location is smaller than that for $L_h$=3.00mm due to extremely smaller needle lift. In contrast to the trend at the high needle lift of $L_h$=3.00mm, the spray cone angle increases with increasing the value of the radial location monotonically. The significant increase

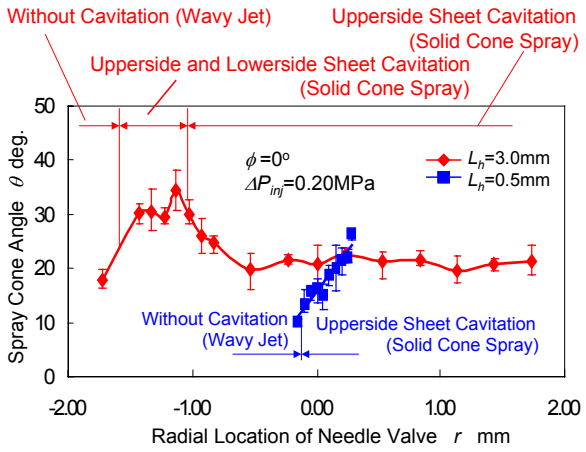


**Figure 3.** Effect of needle lift on spray cone angle. ($\phi$=0°, $\Delta P_{inj}$=0.20MPa)

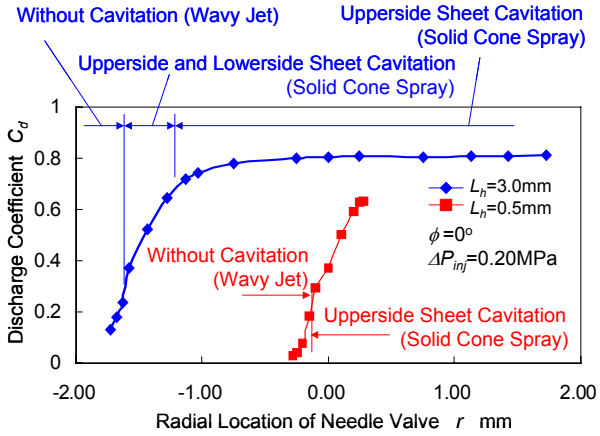


**Figure 5.** Effect of needle lift on discharge coefficient. ($\phi$=0°, $\Delta P_{inj}$=0.20MPa)

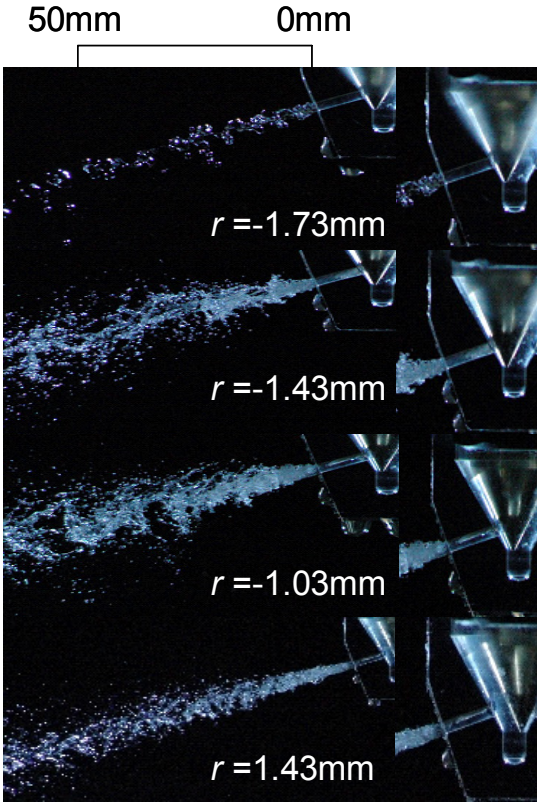


**Figure 4.** Effect of radial location of needle on cavitating flows inside nozzle hole (right photographs) and breakup behavior of liquid jets (left photographs). ($\phi$=0°, $\Delta P_{inj}$=0.20MPa, $L_h$=3.00mm)

of spray cone angle around the nozzle center must be caused by a narrow gap between the needle and the seat because of lower needle lift while the spray cone angle remains constant around the center at higher needle lift.

Figure 4 shows photographs of liquid jets and cavitation bubbles inside the nozzle hole at high needle lift ($L_h$ =3.00mm). Irregular-shaped surfaces are apparent on the liquid column, which are the continuous parts from the exit of the nozzle hole, at the radial location of $r$=-1.73mm, corresponding to a "turbulent breakup" or a "wavy jet" regime because the needle is located near the hole entrance and flow rate of ejecting liquid must be extremely low. Thus cavitating bubbles can not be observed inside the nozzle hole. In contrast, it is indicated that large distance from the entrance of the hole ($r$=-1.43mm, -1.03mm, 1.43mm) leads to significant improvement of atomization due to cavitation. So a "Solid cone spray" regime is obtained, i.e. there exist many large droplets or the liquid column in the center of the spray. On the other hand, few small droplets are appeared in the periphery of the spray. Cavitation bubbles are produced from upperside and lowerside of the hole entrance at the radial location of $r$=-1.43mm. On the contrary, cavitation bubbles are yielded only from upperside of the hole entrance at the radial location of $r$=-1.03mm and 1.43mm. These cavitations, in this study, defined as a "sheet cavitation".

Figure 5 represents the effect of the needle lift on the discharge coefficient at the azimuthal angle of $\phi$=0°. At high needle lift of $L_h$ =3.00mm the discharge coefficient increases with increasing the value of the radial location below the radial location of about $r$=-1.40mm, and then approaches a constant value. Especially the discharge coefficient almost remains relatively constant around the radial location of $r$=0mm. If the needle is in contact with the seat ($r$=-1.80mm), the discharge coefficient must not become zero since the interface curvature of needle is different from that of the seat due to high needle lift. Inclination of the curve becomes relatively significant at the

radial location of $r$=-1.60mm because bubbles of the sheet cavitation are produced from upperside and lower side of the hole entrance. This phenomenon is similar to that which is observed at low needle lift of $L_h$ =0.50mm (about $r$=-0.20mm).

At low needle lift the discharge coefficient increases with the value of increasing radial location monotonically. However the discharge coefficient does not approach a constant value in contrast with high needle lift. Additionally the discharge coefficient at low needle lift is less than that at high needle lift. These results exhibit that thickness of narrow gap between the needle and the seat might influence momentum of the flow, the internal flow structure and production of the cavitating bubbles. In other words, the thickness of the narrow gap might dominate the structure of the liquid jet and primary atomization.

Figure 6 illustrates the effect of the needle lift on the spray cone angle measured at the azimuthal angle of $\phi$=90°. It is noted that the needle is radially positioned in the direction normal to axes of both the nozzle holes at the azimuthal angle $\phi$=of 90°. This figure shows symmetry of the both profiles in contrast to the profiles as represented in Fig. 3. At high needle lift of $L_h$ =3.00mm the spray cone angle remains almost constant as the value of the radial location increases up to $r$=1.00mm. Beyond $r$=1.00mm, the spray cone angle increases significantly, so that the spray cone angle almost reaches maximum value.

The trend of the spray cone angle at high needle lift exhibits two regimes of cavitating flows A and B although the solid cone spray can be observed in both regimes. Figure 7 shows photographs of liquid jets and cavitation bubbles inside the nozzle hole at high needle lift of $L_h$ =3.00mm. There exist bubbles of the vortex cavitation and of the upperside sheet cavitation near the entrance of the hole at radial location of $r$=1.64mm (regime B), while bubbles of the sheet cavitation are only apparent at radial location of $r$=0.14mm (regime A).

At low needle lift of $L_h$ =0.50mm the spray cone angle is larger than that at high needle lift of $L_h$ =3.00mm, although the lower needle lift may lead to the lower discharge coefficient. In addition to the higher spray cone angle, the tendency of the spray cone angle is very complicated in comparison with that at high needle lift or at the azimuthal angle of $\phi$=0°.

Figure 8 exhibits the effect of the injection pressure on spray cone angle at the azimuthal angle of $\phi$=90°. At high injection pressure spray cone angle increases with increasing the value of the radial location up to 0.09mm, and then spray cone angle is diminished significantly. Further increase, the spray cone angle remains constant up to about $r$=0.18mm, and the spray cone angle increases significantly. Finally the spray cone angle reaches almost constant value beyond 0.20mm, which is larger than that between 0.10mm and 0.18mm.

Two different breakup behaviors of liquid jets I and II are obtained as demonstrate in Fig. 9 obtained at the azimuthal angle of $\phi$=90° as follows: one is the solid cone spray/wavy jet regime (regime I) when the needle is located near the center of the nozzle($r$=0mm), and another is the "hollow cone spray" regime (regime II) when the needle is located relatively far from the center of the nozzle ($r$=0.09mm, 0.14mm, 0.34mm). Many large droplets at the periphery of the hollow cone spray are yielded at the end of the conical liquid sheet.

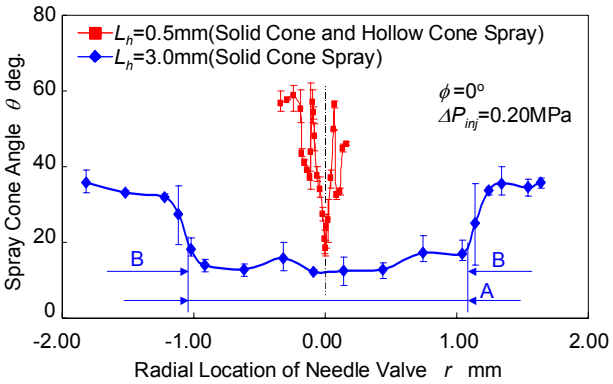


**Figure 6.** Effect of needle lift on spray cone angle. ($\phi$=90°, $\Delta P_{inj}$=0.20MPa)

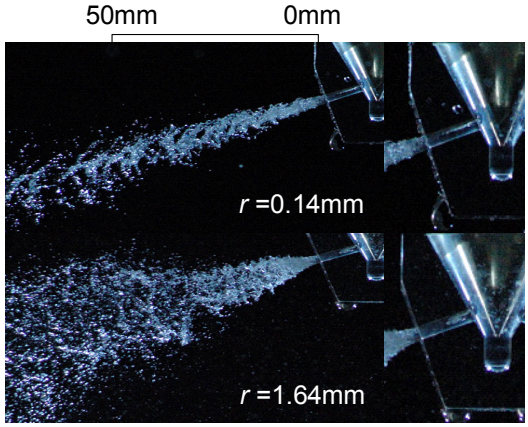


**Figure 7.** Effect of radial location of needle on cavitating flows inside nozzle hole (right photographs) and breakup behavior of liquid jets (left photographs). ($\phi$=90°, $\Delta P_{inj}$=0.20MPa, $L_h$=3.00mm)

Although the injection pressure hardly affects the values of the spray cone angle above 0.15MPa, the spray cone angle is diminished with decreasing the injection pressure below 0.10MPa as shown in Fig. 8. Furthermore cavitation bubbles can not be appeared inside the nozzle hole below the pressure of injection 0.10MPa, so that the wavy jet is observed up to the radial location of 0.09mm. The hollow cone spray is obtained above the radial location of 0.09mm while the cavitating flow can not be observed.

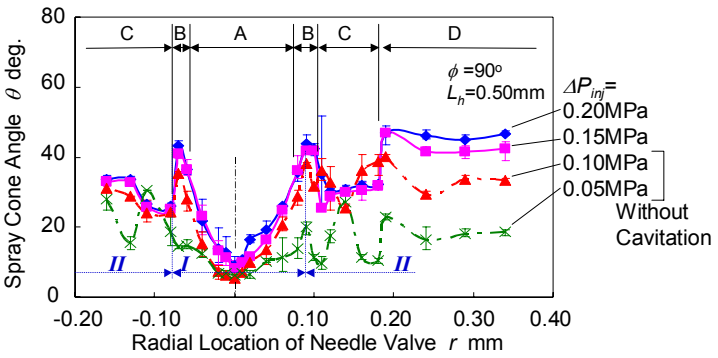


A : Upperside and Lowerside Sheet Cavitation
B : Upperside Sheet Cavitation and Partial Vortex Cavitation
C : Fully Covered Vortex Cavitation D : Partial Vortex Cavitation
*I* : Solid Cone Spray / Wavy Jet *II* : Hollow Cone Spray

**Figure 8.** Effect of injection pressure on spray cone angle. ($\phi$=90°, $L_h$=0.50mm)

Four regimes of cavitating flows represented in Fig. 8 are obtained by similar photographs to Fig. 9. As the needle located near the center of the nozzle (Regime A: upperside and lowerside sheet cavitation, at $r$=0.00mm in Fig. 9), bubble of the vortex cavitation can not be observed but bubbles of the sheet cavitation, which are yielded at upperside and lowerside of the entrance of the hole, can be observed. Regime B is the so-called transient regime (Upperside sheet cavitation and partial vortex cavitation, at $r$=0.09mm in Fig. 9). Short bubble of the vortex cavitation is produced with bubbles of sheet cavitation around the entrance of the hole. The hollow cone spray can not be appeared, before the spray cone angle reaches peak value. As the bubble of the vortex cavitation is elongated and the tip of the bubble penetrates to the exit of the hole, the spray cone angle significantly diminished (Regime C: fully covered vortex cavitation, at $r$=0.14mm in Fig. 9), and the sheet cavitation can not be appeared any more. However the bubble of the vortex cavitation becomes short as the needle is located enough far from a nozzle center in spite of relatively large spray cone angle (Regime D: partial vortex cavitation, at r=0.34mm in Fig. 9).

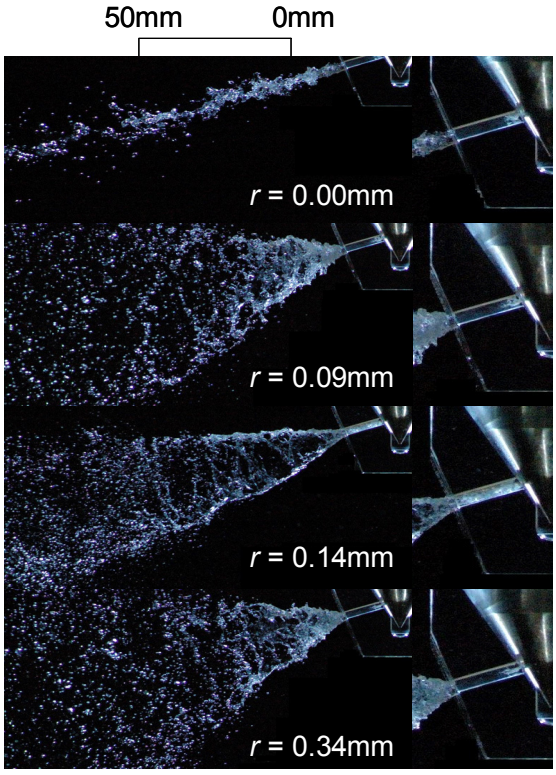


**Figure 9.** Effect of radial location of needle on cavitating flows inside nozzle hole (right photographs) and breakup behavior of liquid jets (left photographs). ($\phi$=90°, $\Delta P_{inj}$=0.20MPa, $L_h$=0.50mm)

Figure 10 represents the effect of injection pressure on the discharge coefficient measured at the azimuthal angle of $\phi$=90°. The discharge coefficient decreases when the value of the radial location of the needle increases from the nozzle center, so that the discharge coefficient reaches minimum value (regime A). In contrast to the regime A, the discharge coefficient increases with increasing the value of the radial location up to peak value (regime B). In this regime volume of sheet cavitation bubble may be reduced gradually while short bubble of the vortex cavitation is produced at the entrance of the hole. Beyond the peak point, the discharge coefficient is diminished because the bubble of the vortex cavitation extends downstream up to the exit of the hole (regime C). Finally the discharge coefficient reaches relatively largest value (regime D) because the bubble of the vortex cavitation is shortened. It is interesting to see from this figure that the radial locations of the regimes A, B, C and D hardly depend on the injection pressure. Additionally the value of the discharge coefficient is less dependent on the

injection pressure except for the regime C, while the spray cone angle is strongly affected by the injection pressure, especially at relatively low injection pressure. These results suggests that the tangential momentum of ejecting liquid must be induced by the eccentricity of the needle and that the ratio of the tangential momentum to axial momentum of ejecting liquid may dominate flow pattern inside the nozzle and structure of the liquid jet strongly.

## Conclusions

An experimental study was carried out to investigate the effects of eccentricity of needle inside a VCO diesel nozzle on internal cavitating flow and primary atomization, so the 10 times large-scaled VCO nozzle was employed. The needle, which was incorporated into the nozzle, was manipulated by a three-dimensional traverse with micrometers.

(1) When the needle is located around nozzle center, the spray cone angle remains constant at high needle lift.
(2) However at low needle lift various behaviors are observed as follows: when the needle is positioned along the nozzle hole (at the azimuthal angle of $0^o$), the significant increase of the spray cone angle is observed around the nozzle center. When the needle is perpendicularly positioned to the nozzle hole (at the azimuthal angle of $90^o$), the tendency of the spray cone angle is very complicated because of cavitating flow behavior inside the nozzle hole, in addition to the relatively high spray cone angle.
(3) At the azimuthal angle of $90^o$ the cavitating flow inside the nozzle hole can be classified into four regimes while two jet regimes, the hollow cone spray regime and the solid cone spray regime, can be obtained at low needle lift.
(4) The radial locations of the four flow regimes hardly depend on the injection pressure. Additionally the value of the discharge coefficient is less dependent on the injection pressure while the spray cone angle is strongly affected by the injection pressure.

## Nomenclature

| | |
|---|---|
| $C_v$ | discharge coefficient |
| $D$ | diameter of nozzle holes |
| $L$ | hole length |
| $L_h$ | needle lift |
| $r$ | radial location of needle |
| $\Delta P_{inj}$ | injection pressure |
| $\phi$ | azimuthal angle of eccentric needle |
| $\theta$ | spray cone angle |

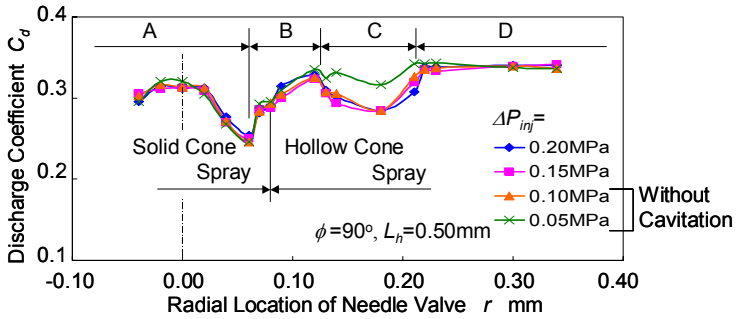


**Figure 10.** Effect of injection pressure on discharge coefficient. ($\phi$=$90^o$, $L_h$=0.50mm)

## References


1. Renner, G, Koyanagi, K. and Maly, R. R., *Proc. the Fourth International Symposium on Diagnostics and Modeling of Combustion in internal Combustion Engines (COMODIA 98)*, pp. 477-482, 1998.
2. Fettes, C., Heimgärtner, C. and Leipertz, A., *The Fifth International Symposium on Diagnostics and Modeling of Combustion in Internal Combustion Engines (COMODIA 2001)*, pp.54-59, 2001.
3. Tsunemoto, H., Ishitani, H., Montajir, R., Hayashi, T., Kitayama, N., *The Fifth International Symposium on Diagnostics and Modeling of Combustion in Internal Combustion Engines (COMODIA 2001)*, pp.528-533, 2001.
4. Kim, J. H., *Ph. D. Thesis*, University of Hiroshima, 2001 (in Japanese).
5. Liverani, L., Arcoumanis, C., Yanagihara, H., Sakata, I. and Omae, K., *Proc. Seventh COMODIA International Symposium on Diagnostics and Modeling of Combustion in internal Combustion Engines*, JSME No.08-202, pp. 453-460.
6. Kim, J. H. Nishida, K. and Hiroyasu H., *The 7th Internal Conference on Liquid Atomization and Spray Systems (ICLASS-'97) Proc.*, pp. 175-182, 1997.
7. T. Oda, S. Kanaike, K. Aoki, Y. Goda and K. Ohsawa, Proc. Of the 12th Annual Conference of ILASS-Asia and the 17th Symposium (ILASS Japan) on Atomization, pp.21-26, 2008.